Reprinted from LANGMUIR, 1992, 8.

Effect of Photopolymerization on the Morphology of Helical Supramolecular Assemblies

Hirotaka Ihara,* Makoto Takafuji, and Chuichi Hirayama

Department of Applied Chemistry, Faculty of Engineering, Kumamoto University, Kumamoto 860, Japan

David F. O'Brien

C. S. Marvel Laboratories, Department of Chemistry, University of Arizona, Tucson, Arizona 85721

Received December 27, 1991. In Final Form: March 19, 1992

A photosensitive chiral lipid was synthesized by introducing 2,4-hexadienoyl groups into a L-glutamate derivative. The lipid in water spontaneously formed single-walled helical aggregates at either 15 or 70 °C (T_c = 51 °C). The lipid assemblies at 15 °C showed a typical blue shift in the absorption of the 2,4-hexadienoyl groups and extremely strong exciton coupling of the absorption (e.g., $[\theta]_{246} = -1.5 \times 10^6$ deg cm^2 dmol^{-1}). These results show that the 2,4-hexadienoyl groups strongly interact in the bilayer interior at temperatures below T_c. Photoirradiation (254 nm) decreased the absorption of 2,4-hexadienoyl groups, and induced a morphological transition from helical lamellar to tubular aggregates at temperatures below T_c and to twisted fibrous aggregates above T_c. The aggregates produced by photoirradiation at 70 °C showed significant stability to temperature change. Binding of methyl orange to the bilayer assembly showed that the morphological transition induced by irradiation at 15 °C occurs with a change of physical states.

Introduction

Since it has been reported by Kunitake et al.[1] and some of us[2] in 1984 that L-glutamate derivatives produced helical bilayer membranes, it has been found that many synthetic chiral amphiphiles could form helical supramolecular assemblies.[3-14] In our studies,[2-4] we have discovered by microscopy some important intermediates in the growth from primitive globular aggregates to helical aggregates for understanding the morphogenesis of helical bilayer assemblies. Fuhrhop et al. discussed the twisting or rolling-up mechanisms of planar bilayer sheets from diastereomeric and enantiomeric lipids.[12,13] Some chiral lipid bilayers show remarkable enhancement of optical activity[5,15-19] and unique dye-binding behavior.[15-17] The bilayer aggregates of lipids **1a**[15] and **1b**[5] show two phase transitions and reversibility between negative and positive chiral states. Several methyl orange binding states were observed in response to the lipid phase transition, T_c.

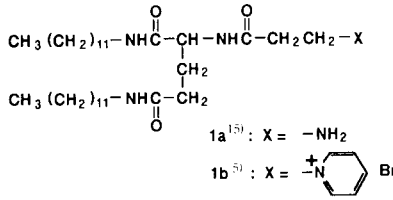

1a[15]: X = $-NH_2$

1b[5]: X =

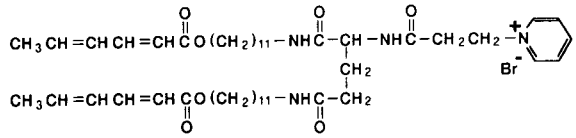

2

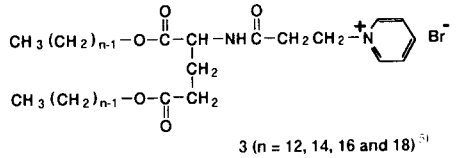

3 (n = 12, 14, 16 and 18)[5]

Since these exceptional properties are closely related to highly oriented amphiphiles in a bilayer assembly, it is interesting to study the effect of polymerization of the properties of these supramolecular assemblies. The polymerization of aqueous bilayer membranes has frequently been achieved by the formation of the assembly from polymerizable lipids followed by polymerization of the assembly.[20,21] In this study, lipid **2** was prepared with the

(1) Nakashima, N.; Asakuma, S.; Kunitake, T. *Chem. Lett.* **1984**, 1709.
(2) Yamada, K.; Ihara, H.; Ide, T.; Fukumoto, T.; Hirayama, C. *Chem. Lett.* **1984**, 1713.
(3) Ihara, H.; Fukumoto, T.; Hirayama, C.; Yamada, K. *Polym. Commun.* **1986**, *27*, 282.
(4) Ihara, H.; Fukumoto, T.; Hirayama, C.; Yamada, K. *Nippon Kagaku Kaishi* **1987**, 543.
(5) Ihara, H.; Yamaguchi, M.; Takafuji, M.; Hachisako, H.; Hirayama, C.; Yamada, K. *Nippon Kagaku Kaishi* **1990**, 1047.
(6) Ihara, H.; Yoshikai, K.; Takafuji, M.; Hirayama, C.; Yamada, K. *Kobunshi Ronbunshu* **1991**, *48*, 327.
(7) Kunitake, T.; Yamada, N. *J. Chem. Soc., Chem. Commun.* **1986**, 655.
(8) Nakashima, N.; Asakuma, S.; Kunitake, T. *J. Am. Chem. Soc.* **1985**, *107*, 509.
(9) Yager, P.; Schoen, P. E.; Davies, C.; Price, R.; Singh, A. *Biophys. J.* **1985**, *107*, 899.
(10) Cho, I.; Park, J.-G. *Chem. Lett.* **1987**, 977.
(11) Georger, J. H.; Singh, A.; Price, R. R.; Schnur, J. M.; Yager, P.; Schoen, P. E. *J. Am. Chem. Soc.* **1987**, *109*, 6169.
(12) Fuhrhop, J.-H.; Schnieder, P.; Boekema, E.; Helfrich, W. *J. Am. Chem. Soc.* **1988**, *110*, 2861.
(13) Fuhrhop, J.-H.; Boettcher, C. *J. Am. Chem. Soc.* **1990**, *112*, 1768.
(14) Yanagawa, H.; Ogawa, Y.; Furuta, H.; Tsuno, K. *J. Am. Chem. Soc.* **1989**, *111*, 4567.
(15) Ihara, H.; Hachisako, H.; Hirayama, C.; Yamada, K. *Liq. Cryst.* **1987**, *2*, 215.
(16) Nakashima, N.; Fukushima, H.; Kunitake, T. *Chem. Lett.* **1981**, 1207.
(17) Nakashima, N.; Ando, R.; Fukushima, H.; Kunitake, T. *J. Chem. Soc., Chem. Commun.* **1982**, 707.
(18) Kunitake, T.; Nakashima, N.; Shimomura, M.; Okahata, Y.; Kano, K. Ogawa, T. *J. Am. Chem. Soc.* **1980**, *102*, 6644.
(19) Nakashima, N.; Morimitsu, M.; Kunitake, T. *Bull. Chem. Soc. Jpn.* **1984**, *57*, 3253.
(20) Ringsdorf, H.; Schlarb, B.; Venzmer, J. *Angew. Chem., Int. Ed. Engl.* **1988**, *27*, 113.

0743-7463/92/2408-1548$03.00/0

Scheme I

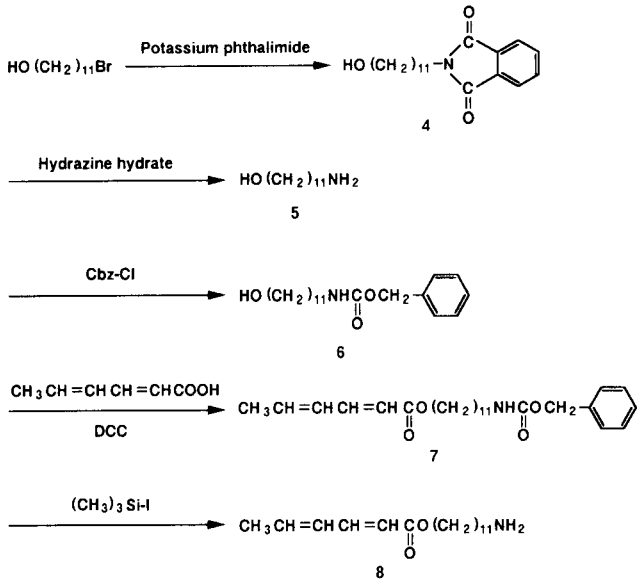

photoreactive 2,4-hexadienoyl (sorboyl) groups associated with the long-chain alkyl groups of **1b**. Sorboyl groups were selected because of their ease of polymerization by UV light and small perturbation of the lipid structure, although it is known that acryloyl and methacryloyl groups are also useful. This paper describes the synthesis of **2** and the morphology of supramolecular assemblies of **2**, both before and after photopolymerization.

Results and Discussion

Molecular Design and Synthesis. The chemical structure of a polymerizable lipid **2** was designed to incorporate a hydrophilic headgroup and two long-chain alkyl groups which are connected to L-glutamic acid by amide bonds, because ester lipids, i.e., **3**, form vesicles in aqueous solutions, whereas the amide-type lipids, i.e., **1a** and **1b**, form stable helical bilayer aggregates.[5] The formation of helical supramolecular assemblies is due to the hydrogen-bonding interactions of amide bonds near the chiral carbon atom.[5] The introduction of polymerizable sorboyl groups at the end of the hydrophobic alkyl chains is far enough from the chiral carbon in order to not reduce the chiral interactions between lipids.

Lipid **2** was obtained via a synthesis similar to that of **1b**.[5] The syntheses are shown in Schemes I and II. 2,4-Hexadienoyl ester of 11-amino-1-undecanol, **8**, was prepared by coupling 11-[*N*-(benzyloxycarbonyl)amino]-1-undecanol, **6**, and 2,4-hexadienoic acid with dicyclohexylcarbodiimide, followed by debenzyloxycarbonylation with iodotrimethylsilane. **6** was obtained from 11-bromo-1-undecanol by the Gabriel method. **8** was coupled with *N*-(benzyloxycarbonyl)-L-glutamic acid using diethylphosphoramide and debenzyloxycarbonylated with iodotrimethylsilane. The alkyl amide **10** was coupled with 3-bromopropionyl chloride, followed by quarternization with pyridine to produce the final compound **2**, which was purified by several recrystallizations to give a single TLC spot (chloroform–methanol, 50:1). The chemical structure was determined by NMR and IR spectroscopies and elemental analysis.

Supramolecular Assemblies of 2. The absorption maximum (λ_{max}) of lipid **2** is 260 nm in ethanol (Figure 1a). The λ_{max} undergoes a hypsochromic shift to 237 nm

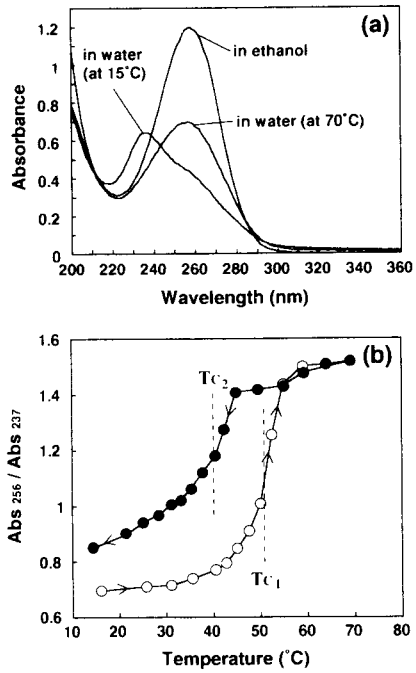

Figure 1. Absorption spectra (a) and the absorbance ratio at 256 and 237 nm (b) for hydrated lipid **2** (0.24 mM). The samples were incubated for 30 min at each temperature. T_{c1} and T_{c2} indicate the lipid phase transition temperatures upon heating and cooling of the samples, respectively.

Scheme II

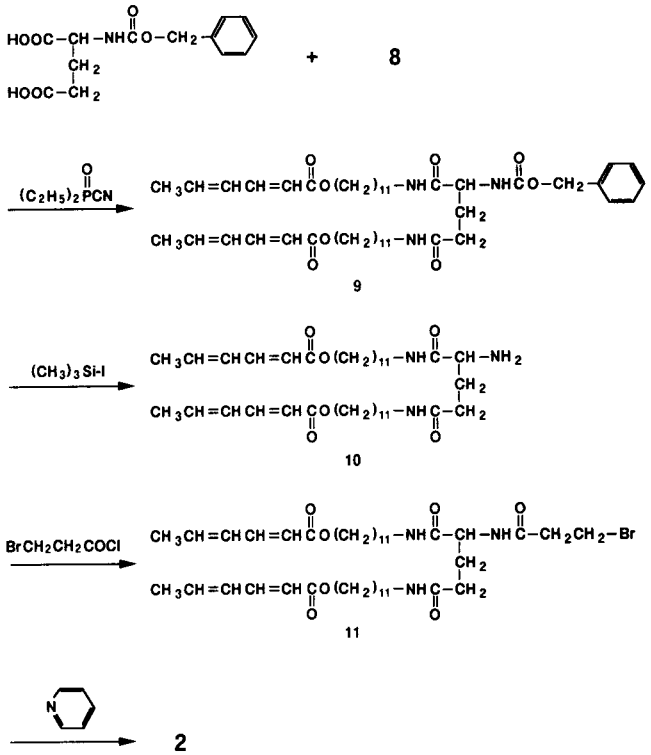

in water at 15 °C (Figure 1a). A similar blue shift was observed in disorboylphosphatidylcholine (**12**) bilayers at temperatures below the T_c by Tyminski et al.[22] The blue shift was proposed to be due to head-to-head stackings of the sorboyl groups. A similar explanation for lipid **2** suggests that it forms highly oriented molecular assemblies in water at 15 °C.

When a suspension of **2** was heated to 70 °C, the λ_{max} shifted to 256 nm and the absorption spectrum was similar

(21) O'Brien, D. F.; Ramaswami, V. In *Encyclopedia of Polymer Science and Engineering*, 2nd ed.; Wiley: New York, 1989; Vol. 17, p 108.

(22) Tyminski, P. N.; Ponticello, I. S.; O'Brien, D. F. *J. Am. Chem. Soc.* **1987**, *109*, 6541.

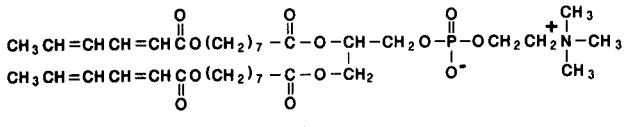

12[25]

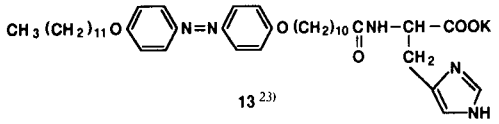

13[23]

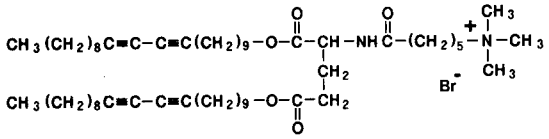

14[28]

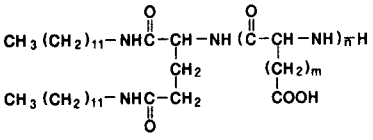

15a[3,4] : m = 1

15b[2,4] : m = 2

to that in ethanol. Figure 1b shows the temperature dependency of the absorbance ratio at 256 nm 237 nm for both the sample heating and cooling processes. Differential scanning calorimetry (DSC) measurements showed that aqueous **2** had a phase transition temperature (peak-maximum temperatures, T_c) of 51 °C (with a shoulder at 56 °C), during the heating scan, and 40 °C during the cooling scan. The DSC data suggest that the aqueous **2** undergoes a gel-to-liquid–crystalline phase transition at the same temperature as the greatest change of the absorbance ratio occurs.

Electron micrographs of air-dried suspensions of **2** provided significant information on its aggregate morphology. Parts a and d of Figure 2 show typical electron micrographs of aqueous **2** aggregates at 15 and 70 °C. Aqueous **2** produced helical supramolecular aggregates which had 40–60-Å-thick strands and were 250–300 Å in diameter across the helices, regardless of temperature. The thickness of the strand is similar to that expected for a molecular bilayer of this lipid. Lipid **1b** appears to form similar single-walled helical bilayer aggregates.[5] Therefore, the introduction of sorboyl groups into lipid **1b** does not significantly perturb the formation of helical supramolecular aggregates. Hydrated **2** forms helical aggregates at temperatures below and above T_c, even though the molecular orientation of the sorboyl groups in the bilayer interior is influenced by the lipid phase transition.

Chiral Properties of Supramolecular Assemblies of 2. Hydrated assemblies of **2** at 15 °C showed extremely strong exciton coupling at wavelength near the absorption of stacked sorboryl groups ($[\theta]_{246} = -1.5 \times 10^6$ and $[\theta]_{231} = 9.0 \times 10^5$ deg cm^2 dmol^{-1} in Figure 3a). The values are much larger than that of the monomeric **2** in ethanol ($[\theta]_{220-300} < -4 \times 10^3$ deg cm^2 dmol^{-1}). Similarly, hydrated lipid **2** at 70 °C shows very small exciton coupling ($[\theta]_{246} = -7.3 \times 10^3$ deg cm^2 dmol^{-1}). The temperature dependencies of $[\theta]_\lambda$ values appear to be related to the lipid phase transition (Figure 3b). These results suggest that head-to-head stackings of sorboyl groups below T_c form *S*-chiral orientation which is not favored at temperatures above T_c.

It has been reported by Kunitake and co-workers that the optical activity of chromophoric lipids is enhanced by bilayer formation.[18,19] However, the amplification factor is dependent on the distance from the chiral center to the chromophoric group as well as the orientation. Consider, for example, the azobenzene chromophore of lipid **13** which is connected to L-histidine through an undecanoyl spacer chain.[23] The distance between the asymmetric carbon atom and the chromopholic group is nearly equal in lipids **13** and **2**. Lipid **13** forms bilayer membranes with large aggregation numbers in water.[23] At temperatures below T_c the aggregates of **13** showed a typical blue shift of 30 nm[23] and a $[\theta]$ value at the absorption of azobenzene groups which was 10–20 times larger than that of the monomeric **13**.[24] The $[\theta]$ value of hydrated lipid **2** was about 200 times larger than in the monomeric state. In order to explain the large effect of the sorboyl groups, the possible three head-to-head stacking states of sorboyl groups are given in Figure 4. The head-to-tail stacking is not considered because it is accompanied by a blue shift. States b and c would exhibit strong chiral interaction, but a is achiral. Figure 3a shows two circular dichroism (CD) bands which are opposite in sign. The positive band is at a shorter wavelength. This CD pattern is the same for a typical example which is observed in the dipole–dipole (*S*-chiral) interaction of the transition moments of dimeric dye molecules bound to chiral poly(α-amino acid)[25] and chiral bilayer membranes.[15] Therefore, state c which is *S*-chiral is consistent with the *S*-chiral cotton effect shown in Figure 3a.

Photoreaction of Supramolecular Assemblies of 2. Photoirradiation of UV light (254 nm) of hydrated lipid **2** assemblies caused a decrease in the absorption of sorboyl groups. Figure 5 shows the time dependence of the UV spectra at 15 °C during the photoreaction which includes an initial decrease of the aggregate absorption at 237 nm followed by a slower decrease of the monomer absorption at 256 nm. The apparent rate constants ($K_{1,app}$) are estimated to be 1.8×10^{-2} and 7.0×10^{-4} s^{-1}, respectively. The UV spectrum indicated by broken lines in Figure 5 is similar to that of lipid **2** at 70 °C. These results indicate that the shoulder around 256 nm at 15 °C is due to non-stacked **2** molecules, which are less photosensitive than head-to-head stacked **2** molecules.

The photoinduced loss of sorboyl groups in hydrated polymerizable lipids is accompanied by polymer formation.[26,27] In general, the polymerization of sorboyl lipid bilayers proceeds above or below T_c,[28] whereas lipid diacetylene bilayers such as **14** can be polymerized only below T_c.[29] Similarly, it was observed that hydrated lipid **2b** assemblies were easily polymerized at temperatures above T_c ($k_{1,app} = 1.0 \times 10^{-2}$ s^{-1} at 70 °C).

Effect of Photoreaction on Morphology. The effect of the UV irradiation on the aggregate morphology was examined by electron microscopy. Figure 2b shows a dried sample of **2** after the UV irradiation for 20 min at 15 °C (90% conversion). The irradiated sample appears to be more nearly tubular than helical, although the diameters (250–300 Å) of the tubules produced are nearly equal to

(23) Kunitake, T.; Ihara, H.; Okahata, Y. *J. Am. Chem. Soc.* **1984**, *105*, 6070.
(24) Ihara, H. Unpublished results.
(25) Hatano, M.; Yoneyama, M.; Sato, Y.; Kawamura, Y. *Biopolymers* **1973**, *12*, 2423.
(26) Frankel, D. A.; Lamparski, H.; Liman, U.; O'Brien, D. F. *J. Am. Chem. Soc.* **1989**, *111*, 9262.
(27) Lamparski, H.; Liman, U.; Barry, J.; Frankel, D. A.; Ramaswami, V.; Brown, M. F.; O'Brien, D. F. *Biochemistry* **1992**, *31*, 685.
(28) O'Brien, D. F.; Liman, U. *Angew. Makromol. Chem.* **1989**, 21.
(29) Kuo, T.; O'Brien, D. F. *Langmuir* **1991**, *7*, 584.

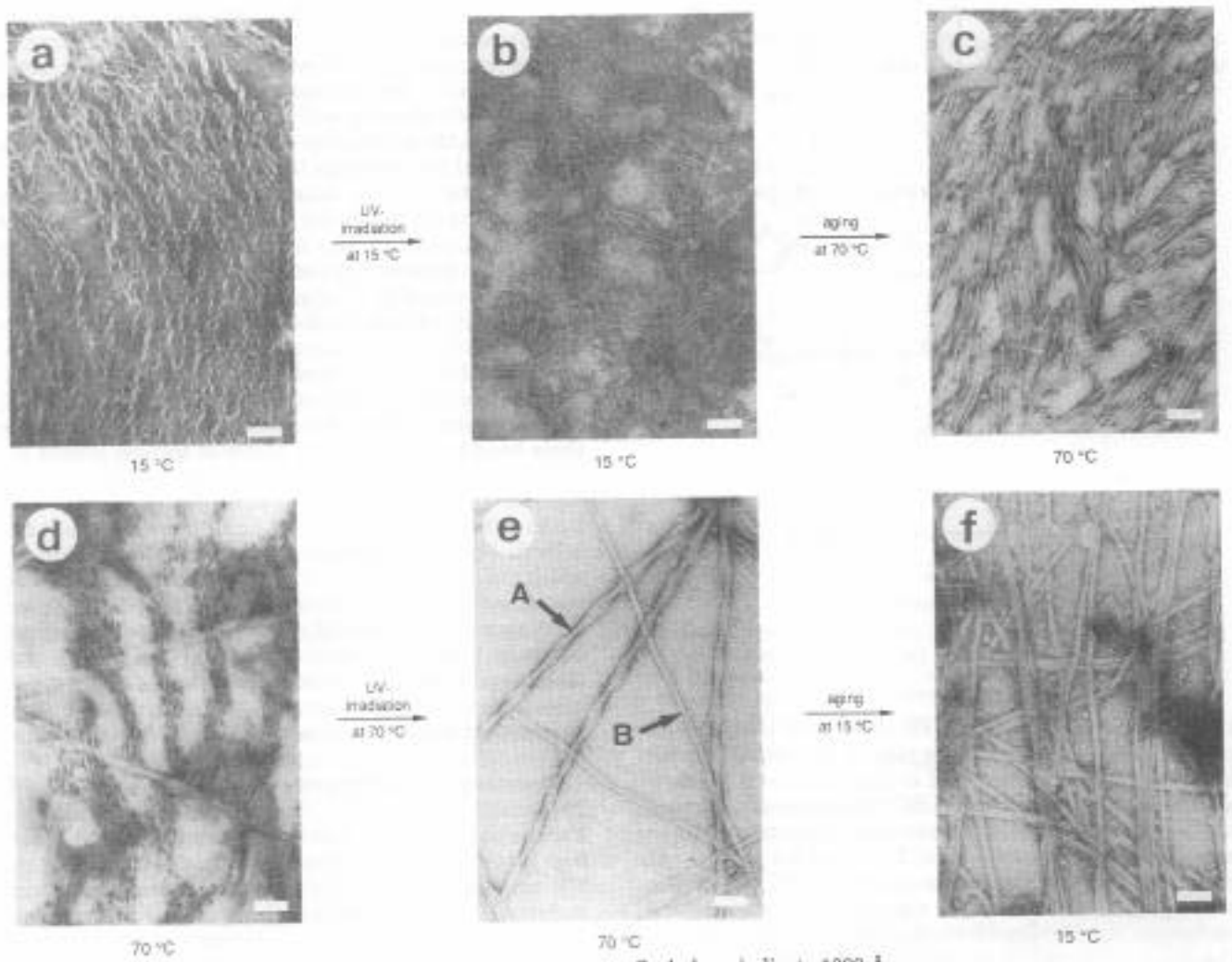

Figure 2. Typical electron micrographs of aqueous 2 aggregates. Scale bars indicate 1000 Å.

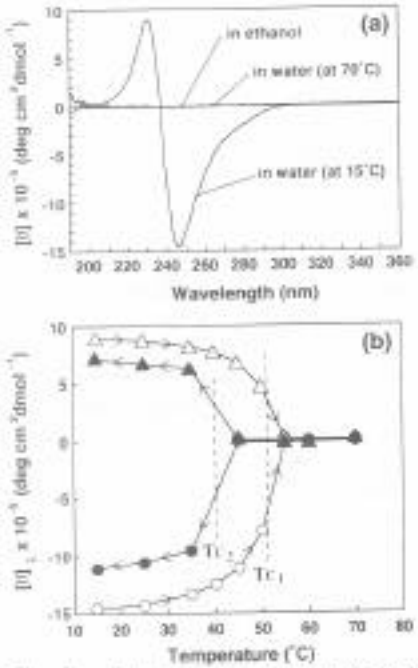

Figure 3. Circular dichroism spectra (a) and temperature dependencies of $[\theta]_r$ values (b) for hydrated lipid 2 (0.24 mM). The circles and triangles show the molecular ellipticity at 246 and 231 nm, respectively.

those of the original helices. This indicates that the curvature of the aggregates is comparable before and after photoreaction. Previously, some of us have suggested that the tubular form of lipid **15a** was a more stable state of helical lamellar bilayers.[2,4] If this is the case, the present experiment of UV irradiation of hydrated **2** at 15 °C causes no significant perturbation of the morphology.

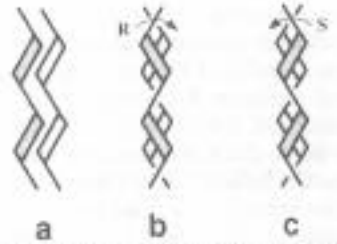

Figure 4. Schematic illustrations of three possibilities of head-to-head stacking of sorboyl groups in aggregates of lipid **2**.

On the other hand, the UV irradiation of hydrate **2** at 70 °C (90% conversion) caused a drastic morphological transition from helical to well-developed and twisted fibrous aggregates (**A** of Figure 2e). The aggregates produced are estimated to be more than 1 μm in length (250–300 Å in diameter). Similar fibrous aggregates were observed for hydrated lipid **15b**, which was produced via formation of double-strand or multistrand helices from untwisted fibrous aggregates as intermediates.[3,4] Untwisted fibrous aggregates with diameters of 130–140 Å are also seen in the case of hydrated lipid **2** aggregates (**B** of Figure 2e).

Interestingly, the aggregates produced by UV irradiation were morphologically stable during temperature changes.

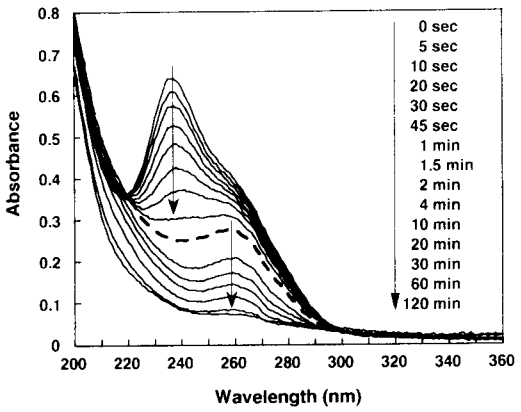

Figure 5. Ultraviolet absorption spectra of hydrated lipid **2** (0.24 mM) as a function of the time of exposure to 254-nm light at 15 °C.

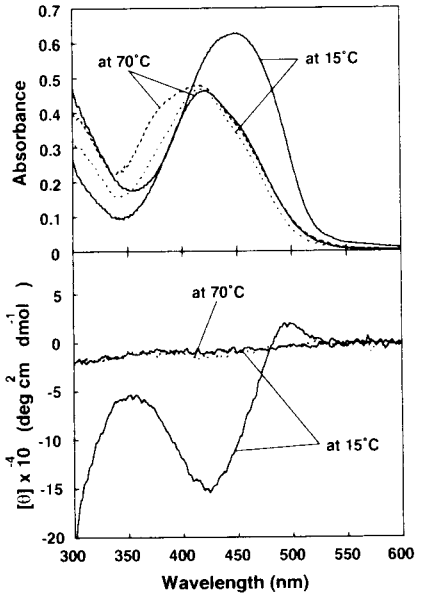

Figure 6. Absorption (a) and CD (b) spectra of a lipid **2**–methyl orange (10:1) mixture in an aqueous solution ([methyl orange] = 0.024 mM): - - -, samples before UV irradiation; · · ·, samples after UV irradiation for 20 min.

As shown in parts c and f of Figure 2, the tubular aggregates at 15 °C or the twisted fibrous aggregates at 70 °C showed no morphological change when they were incubated at 70 or 15 °C for 10 min, respectively. Furthermore, it was observed that the original phase transition at 51 °C was no longer present after UV irradiation for 20 min.

Dye-Binding Behavior. It is well-known that zwitterionic dyes, e.g., methyl orange (MO), can bind to cationic bilayer membranes to give several kinds of spectra, in response to the lipid phase transition.[15][1]–[17] These dye-binding experiments can provide significant information about the microenvironments in chiral lipid bilayers.

Figure 6a shows the absorption spectra of a MO–lipid **2** (1:10) mixture in an aqueous solution. The addition of MO has little effect on the aggregation state of lipid **2**, since no spectral change was observed in the absorption of the lipid sorboyl groups. The addition of MO gave different spectra at 15 or 70 °C with λ_{max} of 450 nm (MO_I) or 420 nm (MO_{II}), respectively. These λ_{max} are similar to those of MO in water and ethanol, respectively. The λ_{max} shift between 450 and 420 nm was thermally reversible and showed temperature dependence similar to that of the sorboyl chromophore (Figures 1b and 3b). The CD spectra showed strong exciton coupling at wavelengths near the absorption of MO, when the sample was at temperatures below T_c (Figure 6b). This indicates that the MO molecules interact strongly with lipid **2** bilayers. The UV irradiation of the lipid **2**–MO mixture at 15 °C caused a significant shift in the λ_{max} from 450 to 420 nm. The spectrum produced is similar to that of the MO_{II}. On the other hand, the UV irradiation of the lipid **2**–MO mixture at 70 °C did not cause a significant spectral change. The effects observed at 15 °C suggest that the MO binding is modified by the photopolymerization of the hydrated lipid **2** assemblies. The UV irradiation at 15 °C may permit the incorporation of MO molecules into the bilayer interior. Therefore, it appears that the UV irradiation at 15 °C induces a significant change of the physical state (from gel to liquid-crystalline states) as well as a morphological change from helical to tubular aggregates.

Summary

The newly synthesized sorboyl glutamate lipid **2** can form helical supramolecular assemblies at temperatures below and above the phase transition temperature, T_c. The properties are dependent upon the sample temperature as follows: (1) At temperatures below T_c, the sorboyl groups interact strongly in the bilayer interior and produce very strong exciton coupling due to the *S*-chiral head-to-head stackings. (2) The UV irradiation of lipid **2** bilayers causes photoreaction of the sorboyl groups at a rate which is 25 times larger in the stacked species (below T_c) than in the nonstacked species. (3) The photoreaction is accompanied by morphological transitions from helical lamellar aggregates to tubular aggregates at temperatures below T_c and to twisted fibrous aggregates above T_c. (4) The dye-binding with methyl orange shows that the morphological transition caused by the photoreaction at temperatures below T_c induces a change in the aggregate structure.

Experimental Section

Methods. All the experiments were carried out under yellow light. Melting points were taken on a micro melting point apparatus. Infrared spectra were recorded on a Perkin-Elmer 1600 series. NMR spectra were taken on a JEOL JNM-GX400. UV absorption spectra were recorded on a Shimadzu UV-160A. Elemental analyses were performed with a Yanaco CHN Corder MT-3. Chloroform and tetrahydrofuran were distilled.

Synthesis. 11-Hydroxyundecyl-1-phthalimide (4). 11-Bromo-1-undecanol (10.4 g, 0.04 mol) and potassium phthalimide (9.3 g, 0.05 mol) were suspended in 100 mL of dimethylformamide and the mixture was stirred for 1 day at 60 °C. A 100-mL portion of water was added to the mixture, and then the resulting precipitates were collected by filtration. The product was recrystallized from methanol to obtain white plates: yield 10.83 g (85%); mp 85–86 °C; IR (KCl) 3548, 3515, 2914, 2849, 1703 cm^{-1}; ^1H NMR ($CDCl_3$) δ 1.05–1.80 (m, 18 H, CH_2), 3.55–3.75 (m, 4 H, CH_2N, CH_2O), 7.60–7.90 (m, 4 H, C_6H_4). Anal. calcd for $C_{19}H_{27}NO_3$: C, 71.89; H, 8.57; N, 4.41. Found: C, 71.59; H, 8.58; N, 4.41.

11-Amino-1-undecanol (5). **4** (11.5 g, 0.03 mmol) was dissolved in 250 mL of ethanol, and 20 mL of hydrazine hydrate was added to the solution. The mixture was stirred for 6 h at reflux temperature, and the precipitates produced were removed by filtration. The filtrate was concentrated in vacuo, and ethyl ether was added. After the precipitates were removed, the filtrate was concentrated in vacuo and the residue was dissolved in the mixture of 20 mL of ethanol and 200 mL of ethyl ether. When the solution was allowed to stand at −20 °C, white powders were obtained: yield 3.99 g (71%); mp 77–78 °C; IR (KCl) 3334, 3300–2500, 2916, 2848, 1612 cm^{-1}; ^1H NMR ($CDCl_3$) δ 0.8–1.6 (m, 18 H, CH_2), 1.59 (s, 2 H, NH_2), 2.55–2.75 (t, 2 H, CH_2N), 3.50–3.70

(t, 2 H, CH_2O). Anal. calcd for $C_{11}H_{25}NO$: C, 70.53; H, 13.45; N, 7.48. Found: C, 70.01; H, 13.59; N, 7.32.

11-[*N*-(Benzyloxycarbonyl)amino]-1-undecanol (6). 5 (5.0 g, 0.027 mol) and triethylamine (3.2 g, 0.03 mol) were dissolved in 50 mL of dimethylformamide and stirred at 0 °C. Carbobenzoxy chloride (3.7 g, 0.022 mol) was added to the solution dropwise over 20 min with stirring at 0 °C. The solution was stirred for 1 h at 0 °C and then for 12 h at room temperature. The solution was washed with 1 N HCl, 1 N NaOH, and water and dried over Na_2SO_4. A 50-mL portion of ethyl ether was added to the solution to give white powders. After the solution was cooled at 0 °C, the precipitates were collected by filtration: yield 5.78 g (60%); mp 71–72 °C; IR (KCl) 3347, 3500–3300, 2922, 2851, 1686, 1530 cm^{-1}; ^1H NMR ($CDCl_3$) δ 1.1–1.6 (m, 18 H, CH_2), 1.74 (s, 1 H, NH), 3.05–3.25 (m, 2 H, CH_2N), 3.50–3.70 (t, 2 H, CH_2O), 5.06 (s, 2 H, $CH_2OC(=O)$), 7.20–7.35 (m, 5 H, C_6H_5). Anal. calcd for $C_{19}H_{31}NO_3$: C, 70.99; H, 9.72; N, 4.36. Found: C, 70.86; H, 9.74; N, 4.35.

11-[*N*-(Benzyloxycarbonyl)amino]undecyl 2,4-Hexadienoate (7). 6 (3.5 g, 0.012 mol), 2,4-hexadienoic acid (1.59 g, 0.014 mol), and 4-(dimethylamino)pyridine (0.29 g, 0.0024 mol) were dissolved in 50 mL of ethyl acetate. Dicyclohexylcarbodiimide (2.79 g, 0.014 mol) was added to the mixture with stirring at 0 °C. After the mixture was stirred for 1 day at room temperature, the dicyclohexylurea produced was removed by filtration. The filtrate was washed with 1 N NaOH and water, and then dried over Na_2SO_4. After the solution was concentrated in vafuo, the residue was recrystallized from methanol at 0 °C to obtain white plates: yield 3.59 g (72%); mp 63–65 °C; IR (KCl) 3342, 2921, 2851, 1708, 1684, 1530 cm^{-1}; ^1H NMR ($CDCl_3$) δ 1.1–1.6 (m, 18 H, CH_2), 1.80–1.84 (d, 3 H, CH_3), 3.05–3.25 (m, 2 H, CH_2N), 4.0–4.2 (t, 2 H, CH_2O), 5.08 (s, 1 H, $CH_2OC(=O)$), 5.70–5.75 (d, 1 H, $=CHC(=O)$), 6.05–6.20 (m, 2 H, CH=CH), 7.15–7.30 (q, 1 H, $CH=CC(=O)$), 7.3–7.4 (m, 5 H, C_6H_5). Anal. calcd for $C_{25}H_{37}NO_4$: C, 72.26; H, 8.97; N, 3.37. Found: C, 71.86; H, 9.00; N, 3.55.

11-Aminoundecyl 2,4-Hexadienoate (8). 7 (1.9 g, 0.0046 mol) was dissolved in 15 mL of chloroform. The solution was cooled to 0 °C, and iodotrimethylsilane (1.4 g, 0.0069 mol) was added to the solution. The solution was stirred for 3 h at 0 °C. A 1-mL portion of methanol was added to the solution and stirred for 5 min. A 15-mL portion of hexane was added to the reaction mixture, and the precipitates were collected by filtration and recrystallization from benzene to obtain white powders: yield 1.21 g (93%); mp 139–141 °C; IR (KCl) 3200–2800, 2926, 2854, 1706 cm^{-1}; ^1H NMR ($CDCl_3$) δ 1.2–1.45 (m, 16 H, CH_2), 1.6–1.7 (m, 2 H, CH_2), 1.84–1.86 (d, 3 H, CH_3), 3.1–3.14 (t, 2 H, CH_2N), 4.1–4.15 (t, 2 H, CH_2O), 5.75–5.8 (d, 1 H, $=CHC(=O)$), 6.1–6.25 (m, 2 H, CH=CH), 7.2–7.28 (q, 1 H, $CH=CC(=O)$). Anal. calcd for $C_{17}H_{31}NO_2I$: C, 50.00; H, 7.65; N, 3.43. Found: C, 49.70; H, 8.00; N, 3.26.

***N*′,*N*″-Bis[11-(sorboyloxy)undecyl]-*N*-(benzyloxycarbonyl)-L-glutamide (9).** *N*-(Benzyloxycarbonyl)-L-glutamic acid (0.53 g, 0.0019 mol), triethylamine (0.69 g, 0.0068 mol), and 8 (1.3 g, 0.0046 mol) were mixed in 30 mL of tetrahydrofuran. A 10-mL portion of tetrahydrofuran solution containing diethyl cyanophosphonate (1.11 g, 0.0068 mol) was added to the mixture at 0 °C. After being stirred for 1 day at room temperature, the solution was washed with 1 N NaOH, 1 N HCl, and water. The solution was dried over Na_2SO_4 and concentrated in vacuo. The residue was recrystallized from methanol to give white powders: yield 0.63 g (41%); mp 113–116 °C; IR (KCl) 3298, 2921, 2851, 1707, 1689, 1647 cm^{-1}; ^1H NMR ($CDCl_3$) δ 1.2–1.4 (m, 28 H, CH_2), 1.4–1.55 (m, 4 H, CH_2), 1.6–1.72 (m, 4 H, CH_2), 1.84–1.86 (d, 6 H, CH_3), 1.9–2.1 (m, 2 H, CH_2*C), 2.25–2.4 (m, 2 H, CH_2C*C), 3.15–3.27 (m, 4 H, CH_2N), 4.1–4.14 (t, 4 H, CCH_2O), 4.16–4.18 (m, 1 H, *CH), 5.1 (s, 2 H, CH_2C_6), 5.75–5.79 (d, 2 H, $=CHC(=O)$), 6.14–6.19 (m, 4 H, CH=Ch), 7.2–7.3 (q, 2 H, $CH=CC(=O)$), 7.3–7.38 (m, 5 H, C_6H_5). Anal. calcd for $C_{47}H_{73}N_3O_8$: C, 69.86; H, 9.11; N, 5.20. Found: C, 69.03; H, 9.14; N, 5.22.

***N*′,*N*″-Bis[11-(sorboyloxy)undecyl]-L-glutamide (10).** Purified 9 (0.6 g, 0.74 mmol) was dissolved in 10 mL of chloroform, and 0.3 g (1.5 mmol) of iodotrimethylsilane was added with stirring at 0 °C. The stirring was continued for 1 h at 0 °C and for 1 day at room temperature. Methanol (1 mL) was added to the reaction mixture, and it was concentrated in vacuo. Ethyl ether was added to the residue, and the solution was allowed to stand at −20 °C to obtain a brown oil. The product was used for the next procedure without further purification.

***N*′,*N*″-Bis[11-(sorboyloxy)undecyl]-*N*-(bromopropionyl)-L-glutamide (11).** Crude 10 (ca. 0.7 mmol) was dissolved in distilled tetrahydrofuran, and triethylamine (0.18 g, 1.5 mmol) was added to the solution. 3-Bromopropionyl chloride (0.25 g, 1.5 mmol) dissolved in tetrahydrofuran (10 mL) was added dropwise to the solution with stirring at 0 °C. After the solution was stirred for 2 h at 0 °C, ethyl acetate (50 mL) and ethyl ether (20 mL) were added. The mixture was washed with 1 N HCl, 1 N NaOH, and water and dried over Na_2SO_4. The solution was concentrated in vacuo. Hexane was added to the residue, and the precipitates produced were collected and washed with ethyl ether: yield 0.28 g (ca. 50%); mp 119–123 °C; IR (KCl) 3328, 2924, 2852, 1708, 1637, 1540 cm^{-1}; ^1H NMR ($CDCl_3$) δ 1.2–1.4 (m, 28 H, CH_2), 1.4–1.55 (m, 4 H, CH_2), 1.6–1.75 (m, 4 H, CH_2), 1.84–1.86 (d, 6 H, CH_3), 1.95–2.15 (m, 2 H, CH_2*C), 2.25–2.5 (m, 2 H, CH_2C*C), 2.7–2.85 (m, 2 H, CH_2CBr), 3.2–3.3 (m, 4 H, CH_2N), 3.65–3.85 (m, 2 H, CH_2Br), 4.1–4.14 (t, 4 H, CCH_2O), 4.35–4.35 (m, 1 H, *C), 5.75–5.79 (d, 2 H, $=CHC(=O)$), 6.1–6.25 (m, 4 H, CH=CH), 7.2–7.3 (q, 2 H, $CH=CC(=O)$). Anal. calcd for $C_{42}H_{70}N_3O_7Br$: C, 62.36; H, 8.72; N, 5.19. Found: C, 63.25; H, 8.66; N, 5.28.

***N*′,*N*″-Bis[11-(sorboyloxy)undecyl](pyridinium-*N*-ylpropionyl)-L-glutamide Bromide (2).** 11 (0.14 g, 0.16 mmol) was dissolved in pyridine (3 mL), and the solution was kept for 1 day at 50 °C. Ethyl ether (50 mL) was added to give light orange powders. The product was recrystallized from etahnol–ethyl ether (10 mL/40 mL): yield 0.11 g (75%); mp 116–125 °C; IR (KCl) 3300, 2916, 2850, 1708, 1654 cm^{-1}; ^1H NMR ($CDCl_3$) δ 1.2–1.4 (m, 28 H, CH_2), 1.4–1.55 (m, 4 H, CH_2), 1.58–1.72 (m, 4 H, CH_2), 1.84–1.86 (d, 6 H, CH_3), 1.95–2.15 (m, 2 H, CH_2*C), 2.25–2.5 (m, 2 H, CH_2C*C), 3.1–3.2 (m, 4 H, CH_2N), 3.3–3.4 (m, 2 H, $CH_2C(Py)$), 4.1–4.14 (t, 4 H, CCH_2O), 4.2–4.3 (m, 1 H, *C), 5.1–5.2 (m, 2 H, CH_2Py), 5.75–5.79 (d, 2 H, $=CHC(=O)$), 6.1–6.25 (m, 4 H, CH=CH), 7.2–7.3 (q, 2 H, $CH=CC(=O)$), 8.02–8.08 (t, 2 H, *m*-Py), 8.38–8.48 (t, 1 H, *p*-Py), 9.3–9.4 (d, 2 H, *o*-Py). Anal. calcd for $C_{47}H_{75}N_4O_7Br$: C, 63.57; H, 8.51; N, 6.31. Found: C, 62.58; H, 8.34; N, 6.05.

Lipid Membrane Preparation. The lipid 2 (2.4 μmol) was hydrated with 10 mL of deionized water at 70 °C, and then the suspension was kept at 0 °C for 1 h. The suspension was warmed to room temperature to obtain an optically clear sample (0.24 mM).

Photopolymerization of the Lipid 2 Membranes. Aqueous samples of 2 (0.24 mM) were put into a quartz cell with a 1-mm path length, and the cell was capped tightly. The samples were irradiated with a low-pressure mercury lamp at a distance of 10 cm for selected times and temperatures.

Differential Scanning Calorimetry. DSC thermograms of the sample solution (22.5 mM) were obtained using a heating and cooling rate of 1 °C min^{-1} with a Seiko I & E SSC-580 with a DSC-10 instrument.

Absorption and Circular Dichroism Measurements. The samples in a 1-mm quartz cell were incubated for 30 min at selected temperatures. The absorption and CD spectra were measured with Shimadzu UV160A and JASCO J-500C spectrophotometers, respectively.

Transmission Electron Microscopy. Transmission electron micrographs were recorded by using a JEOL 2000FX. The aqueous samples (5.6×10^{-4} M) were spotted on carbon-coated copper grids. After the samples were aird-dried at each temperature, they were stained with 2% aqueous uranyl acetate.

Registry No. 2, 140875-98-5; 2 (homopolymer), 140876-05-7; 4, 99824-42-7; 5, 27780-89-8; 6, 140875-99-6; 7, 140876-00-2; 8, 140876-01-3; 9, 140876-02-4; 10, 140876-03-5; 11, 140876-04-6; MO, 547-58-0; Cbz-Cl, 501-53-1; $HO(CH_2)_{11}Br$, 1611-56-9; $CH_3(CH=CH)_2CO_2H$, 110-44-1; $Br(CH_2)_2COCl$, 15486-96-1; *N*-(benzyloxycarbonyl)-L-glutamic acid, 1155-62-0; pyridine, 110-86-1; potassium phthalimide, 1074-82-4.